

# Non-Gaussianity of the density distribution in accelerating universes II:N-body simulations

Takayuki Tatekawa<sup>†,‡</sup> and Shuntaro Mizuno<sup>||</sup>

<sup>†</sup>The center for Continuing Professional Development, Kogakuin University, 1-24-2 Nishi-shinjuku, Shinjuku, Tokyo 163-8677, JAPAN

<sup>‡</sup>Advanced Research Institute for Science and Engineering, Waseda University, 3-4-1 Okubo, Shinjuku, Tokyo 169-8555, JAPAN

<sup>||</sup> Research Center for the Early Universe (RESCEU), School of Science, University of Tokyo, 7-3-1 Hongo, Bunkyo, Tokyo 113-0033, JAPAN

**Abstract.** We explore the possibility of putting constraints on dark energy models with statistical property of large scale structure in the non-linear region. In particular, we investigate the  $w$  dependence of non-Gaussianity of the smoothed density distribution generated by the nonlinear dynamics. In order to follow the non-linear evolution of the density fluctuations, we apply N-body simulations based on  $P^3M$  scheme. We show that the relative difference between non-Gaussianity of  $w = -0.8$  model and that of  $w = -1.0$  model is 0.67% (skewness) and 1.2% (kurtosis) for  $R = 8h^{-1}$  Mpc. We also calculate the correspondent quantities for  $R = 2h^{-1}$  Mpc, 3.0% (skewness) and 4.5% (kurtosis), and the difference turn out to be greater, even though non-linearity in this scale is so strong that the complex physical processes about galaxy formation affect the galaxy distribution. From this, we can expect that the difference can be tested by all sky galaxy surveys with the help of mock catalogs created by selection functions, which suggests that non-Gaussianity of the density distribution potentially plays an important role for extracting information on dark energy.

PACS numbers: 02.60.Cb, 45.50.Jf, 95.36.+x, 98.65.Dx

## 1. Introduction

The formation of large scale structure in the Universe is a central element of astrophysics. The key idea in understanding the formation of the structure in the Universe is gravitational instability [1, 2, 3, 4]. Roughly stated, if the material in the Universe distributed irregularly, then the overdense regions provide extra gravitational attraction, draw material toward them and become more overdense. At present, this simple picture dramatically succeeds in explaining what is observed and current attention is focused entirely on the details of the gravitational instability process which strongly depends on the cosmological models.

One of the useful means to extract the detail of structure formation is the statistical property of observable quantities. Among various statistical quantities, the density probability distribution function (PDF) of the density contrast plays a very important role because it includes information of non-Gaussianity. In the standard picture, the primordial density fluctuations originated from quantum fluctuations are stretched to large comoving scales during the inflation phase and assumed to be random Gaussian [5]. It is, however, well known that even though the density fluctuations remain Gaussian in the linear regime, it significantly deviates from Gaussian once the non-linear stage is reached [6, 7]. Since structure formation is competition between the cosmic expansion and gravity, the growth of the density contrast as well as the evolution of its statistical quantities are intimately tied to the cosmic expansion law of the Universe.

On the other hand, according to recent observations for type Ia Supernovae [8], the expansion of the Universe is accelerating. Combining measurements of Cosmic Microwave Background Radiation [9] and recent galaxy redshift survey [10], we are forced to recognize the existence of a cosmological constant, or kind of dark energy whose value is almost the same order of magnitude as the present density of the Universe [11]. (For reviews about the cosmological constant problem, see [12].) From the phenomenological viewpoint, in order to clarify the property of dark energy, it is important to constrain the effective equation of state of dark energy  $w$  by observations. Even though we have obtained the constraint as  $w < -0.90$  (95 % confidence limit assuming  $w \geq -1$ ) [11] by combining WMAP data with other astronomical data, in order to pin down the value of  $w$ , it is necessary to propose other independent and complementary methods.

For this purpose, as stated at the beginning, we suppose the statistical property of large scale structure of the Universe is helpful. Actually, we were the first to analyze the  $w$ -dependence of non-Gaussianity of the PDF of the smoothed density contrast in [13] where we considered simple constant- $w$  dark energy models with  $w = -0.5, -0.8, -1.0, -1.2$ . (The case for the cosmological constant ( $w = -1$ ) had already been considered in such as [14, 15, 16].) There, in order to see the effects of the non-linear dynamics analytically, as a first step, we adopted Lagrangian linear perturbation [17, 18, 19] which describes the evolution of the density fluctuation in the quasi-nonlinear region better than second order Eulerian perturbation [20, 21].

As a natural extension to the previous one, in order to go into the strongly nonlinear region where the difference of non-Gaussianity depending on  $w$  is expected to be large, numerical simulations seem to be necessary. Even though the simulations including dark energy are important, because of computational expense of the simulations, the first simulations including dark energy other than the cosmological constant appeared only in 2003. By now the aim of N-body simulations in the presence of dark energy are limited to the mass function of dark matter halo [22, 23, 24] as well as the matter power spectrum [25]. Therefore, in this paper, we analyze the  $w$ -dependence of non-Gaussianity of the PDF of the smoothed density contrast with N-body simulations to cover the strongly nonlinear region where the results of [13] remain invalid.

This paper is organized as follows. In section 2, we briefly summarize the effects of dark energy on the structure formation scenario and define the quantities which are necessary to estimate non-Gaussianity of the density distribution in section 3. The set up and results of N-body simulations are described in Section 4 and Section 5, respectively. Section 6 is devoted to conclusions.

## 2. Effects of dark energy

Here, we briefly summarize the effects of dark energy. We consider almost the same situation as our previous paper [13] where we assumed the following facts;

(a) As for matter components, we consider (cold dark) matter and dark energy, i.e.  $\rho_{\text{tot}} = \rho_m + \rho_{\text{DE}}$ , where  $\rho_{\text{tot}}$ ,  $\rho_m$  and  $\rho_{\text{DE}}$  are total energy density of matter, each component of energy density of matter and dark energy, respectively.

(b) Dark energy interacts with matter only gravitationally, i.e. the energy conservation of matter and dark energy holds independently.

(c) The effective equation of state of dark energy  $w$  is constant for simplicity, even though in principle, we can relax this condition.

(d) Curvature of the Universe is negligible, i.e. ( $\mathcal{K} = 0$ ).

Then, the background Friedmann equation can be written as

$$H^2 = H_0^2 \left[ \Omega_{m0} a^{-3} + \Omega_{DE0} a^{-3(w+1)} \right], \quad (1)$$

where  $a$  is a scale factor of the Universe,  $H = \dot{a}/a$  is its Hubble parameter. We have also defined the density parameters for matter and dark energy:

$$\Omega_{(m, DE)} \equiv \frac{8\pi G}{3H^2} \rho_{(m, DE)}. \quad (2)$$

The subscripts 0 denote that the corresponding quantities are evaluated at the present time. From Eq. (1), the effects of dark energy affect the background cosmic expansion, which depends on the effective equation of state of dark energy  $w$ .

Since structure formation is described as competition between the cosmic expansion and gravity, the change of the cosmic expansion modifies the growth of the fluctuations. In the following, we summarize the results obtained in structure formation, limiting to the linear perturbation theory, for simplicity.

In the comoving coordinates, the Poisson equation is given by

$$\nabla^2\Phi = \frac{3}{2}\Omega_m H^2 a^2 \delta_m, \quad (3)$$

where  $\Phi$  is the gravitational potential in the comoving coordinates,  $\delta_m \equiv (\rho_m - \rho_{mb})/\rho_{mb}$  is the density fluctuation of matter,  $\rho_{mb}$  is the background density of matter.

Combined with the continuity equation and Euler equation, the growth equation of the matter perturbation can be obtained

$$\ddot{\delta}_m + 2H\dot{\delta}_m - \frac{3}{2}H^2\Omega_m\delta_m = 0, \quad (4)$$

where the dot denotes a time derivative.

Therefore the growth of large scale structure depends on the background cosmic expansion law and it provides one of the constraints to the property of dark energy.

Strictly speaking, in dark energy models with a dynamical field, one might wonder whether perturbations of the field might affect the growth of structure. However, since calculations of the galaxy power spectrum in such models suggest that the field is essentially smooth on these scales [26, 27], we assume that the perturbations of the field do not impact structure on these scales.

### 3. Non-Gaussianity of the density distribution

In what follows, since we are usually interested in the density fluctuations of matter, we will omit the subscript  $m$  unless otherwise stated. In order to analyze the statistical properties of the density contrast, we introduce a one-point probability distribution function of the density fluctuation field  $P(\delta)$  (PDF of the density fluctuation) which denotes the probability of obtaining the value  $\delta$ . If  $\delta$  is a random Gaussian field, the PDF of the density fluctuation is determined completely as

$$P(\delta) = \frac{1}{(2\pi\sigma)^{1/2}} e^{-\delta^2/2\sigma^2}, \quad (5)$$

where  $\sigma^2 \equiv \langle (\delta - \langle \delta \rangle)^2 \rangle$  is the dispersion and  $\langle \rangle$  denotes the spacial average.

At initial,  $\delta$  is often treated as a random Gaussian field as a result of the generic prediction of inflationary scenario [28]. In the linear perturbation theory, Gaussianity of  $\delta$  is completely conserved if we start with a Gaussian initial condition, because each Fourier mode evolves independently according to the growth law Eq. (4).

Once nonlinear terms are considered, however, the PDF deviates from the initial Gaussian shape. The point is that  $\delta$  is constrained to have a value  $\delta \geq -1$ , otherwise the energy density  $\rho$  would be negative [4]. The Gaussian distribution (5) always assigns non-zero probability to the unphysical regions with  $\delta < -1$ . The error is negligible when  $\sigma$  is small because the probability of obtaining the value  $\delta < -1$  is then very small, but, as fluctuations enter the strongly nonlinear regime with  $\sigma \sim 1$ , this error must become so important that the Gaussian distribution is only a poor approximation to the real distribution. What happens is that, as fluctuations evolve, mode-coupling effects cause

the initial distribution to skew, generating a long tail at high  $\delta$  while they are bounded at  $\delta = -1$ .

If the PDF deviates from Gaussian distribution, the cumulants of the one-point PDF of the density fluctuation field whose orders are higher than two become nonzero. Especially, the third and fourth order cumulants, which are defined as  $\langle \delta^3 \rangle_c \equiv \langle \delta^3 \rangle$ ,  $\langle \delta^4 \rangle_c \equiv \langle \delta^4 \rangle - 3\sigma^4$  mean the display asymmetry and non-Gaussian degree of “peakiness”, respectively, for a given dispersion.

Since it is known that the scaling  $\langle \delta^n \rangle_c \propto \sigma^{2n-2}$  holds for weakly non-linear region, if we consider the gravitational clustering from Gaussian initial conditions [30], we introduce the following higher-order statistical quantities [1, 2]:

$$\begin{aligned} \text{skewness} : \gamma &= \frac{\langle \delta^3 \rangle_c}{\sigma^4}, \\ \text{kurtosis} : \eta &= \frac{\langle \delta^4 \rangle_c}{\sigma^6}. \end{aligned}$$

The merit of adopting these definitions is, as stated above, that they are constants in extremely weakly nonlinear stage which are given by Eulerian linear and second-order perturbation theory [1, 30]. For example, in Einstein-de Sitter Universe, the skewness and kurtosis are given by

$$\begin{aligned} \gamma &= \frac{34}{7} + \mathcal{O}(\sigma^2), \\ \eta &= \frac{60712}{1323} + \mathcal{O}(\sigma^2). \end{aligned}$$

Even though it is shown that the skewness in weakly nonlinear region does not deviate much from 34/7 in several dark energy models [31, 32, 33], the region we can observe is nearer and the nonlinearity becomes stronger. Therefore, in the following, we concentrate on these quantities by analyzing the nonlinear evolution of the fluctuations.

It is worth noting that in the previous paper [13], we used other definitions for the skewness and kurtosis which are based on [6] in which  $\langle \delta^n \rangle_c$  is divided by  $\sigma^n$ . The ones in the previous definition should be divided by  $\sigma$  and  $\sigma^2$  for the skewness and kurtosis, respectively, to obtain the ones in the present definition.

#### 4. N-body simulations

In our previous paper [13], in order to analyze the non-linear dynamics, we applied Lagrangian perturbation theory where we can extract the quasi-nonlinear nature even if we consider only the linear order. Since we could obtain the naive  $w$ -dependence of non-Gaussianity of the density distribution in the weakly nonlinear region, as a natural extension, in this paper, we apply cosmological N-body simulations in order to obtain quantitatively plausible predictions.

Below we describe the N-body codes, initial conditions, parameter choices and technical details of simulations. The results themselves are reported in Section 5.

The numerical algorithm is applied by particle-particle particle-mesh ( $P^3M$ ) method whose code had been originally written by Bertschinger [34]. The initial

**Table 1.** The relation between  $w$  and  $\sigma_8$ . This relation is derived from Eq. (11).

$w$	$\sigma_8$
-0.5	0.56967
-0.8	0.663688
-0.9	0.698358
-1.2	0.813615

Gaussian fluctuation is generated by COSMICS [35]. Until the quasi-nonlinear regime, COSMICS evolves the fluctuation within the scheme of Lagrangian linear perturbation. Then, we start N-body simulations at  $z \simeq 30$ .

For N-body simulations, we set the parameters as follows:

$$\begin{aligned}
 \text{Number of particles} &: N = 128^3, \\
 \text{Box size} &: L = 128h^{-1}\text{Mpc} \quad (\text{at } a = 1), \\
 \text{Softening length} &: \varepsilon = 50h^{-1}\text{kpc} \quad (\text{at } a = 1).
 \end{aligned}$$

The cosmological parameters at the present time ( $a = 1$ ) are given by WMAP [11]:

$$\Omega_m = 0.28, \quad (6)$$

$$\Omega_{DE} = 0.72, \quad (7)$$

$$H_0 = 73 \text{ [km/s/Mpc]}, \quad (8)$$

$$\sigma_8 = 0.74. \quad (9)$$

For dark energy models, we set several equations of state.

$$p_{DE} = w\rho_{DE}, \quad (w = -0.5, -0.8, -0.9, -1.0, -1.2), \quad (10)$$

where  $w = -1.0$  corresponds to the cosmological constant. Even though  $w = -0.5$  has already been excluded and the strong energy condition is violated in the case of  $w = -1.2$ , we calculate these cases as well for comparison.

According to the recent clustering results of XMM-Newton soft X-ray sources, the parameter  $\sigma_8$  depends on  $w$  [36]. The relation between  $\sigma_8$  and  $w$  can be fit by

$$\sigma_8 = 0.34(\pm 0.01)\Omega_m^{-\gamma(\Omega_m, w)}, \quad (11)$$

$$\gamma(\Omega_m, w) = 0.22(\pm 0.04) - 0.40(\pm 0.05)w - 0.052(\pm 0.040)\Omega_m. \quad (12)$$

Using this relation, we compute  $\sigma_8$  for several  $w$  cases (Table 1).

In order to avoid the divergence of the density fluctuation in the limit of large  $k$  and since the observed distribution is intrinsically discrete, it is necessary to consider the density field  $\rho(\mathbf{x}; R)$  at the position  $\mathbf{x}$  smoothed over some scale  $R$ , which is related to the unsmoothed density field  $\rho(\mathbf{x})$  as

$$\begin{aligned}
 \rho(\mathbf{x}; R) &= \int d^3\mathbf{y} W(|\mathbf{x} - \mathbf{y}|; R) \rho(\mathbf{y}) \\
 &= \int \frac{d^3\mathbf{k}}{(2\pi)^3} \tilde{W}(kR) \tilde{\rho}(\mathbf{k}) e^{-i\mathbf{k}\cdot\mathbf{x}}, \quad (13)
 \end{aligned}$$

where  $W$  denotes a window function and  $\tilde{W}$  and  $\tilde{\rho}$  represent the Fourier transforms of the corresponding quantities. In this paper, after the calculations, we perform smoothing with a spherical top-hat window function,

$$\tilde{W} = \frac{3(\sin x - x \cos x)}{x^3}, \quad (14)$$

which yield the density fluctuation  $\delta(\mathbf{x}; R)$  at the position  $\mathbf{x}$  smoothed over the scale  $R$ . For simplicity we use  $\delta$  to denote  $\delta(\mathbf{x}; R)$  unless otherwise stated.

It is also shown that for the case of smoothing with the spherical top-hat filter with radius  $R$ , in the weakly nonlinear region, the skewness and kurtosis of the density distribution can be obtained analytically for a given cosmology. For example, in Einstein-de Sitter Universe, they are given as

$$\begin{aligned} \gamma &= \frac{34}{7} + \frac{d \log \sigma^2(R)}{d \log R} + \mathcal{O}(\sigma^2), \\ \eta &= \frac{60712}{1323} + \frac{62}{3} \frac{d \log[\sigma^2(R)]}{d \log R} + \frac{7}{3} \left( \frac{d \log[\sigma^2(R)]}{d \log R} \right)^2 \\ &\quad + \frac{2}{3} \frac{d^2 \log[\sigma^2(R)]}{d(\log R)^2} + \mathcal{O}(\sigma^2). \end{aligned}$$

In our previous paper [13], we choose the smoothing scale  $R$  as a rather large value ( $8h^{-1}$  Mpc), because Lagrangian linear perturbation cannot approximate the strongly nonlinear regime well because of shell-crossing or caustics formation. Since our present analysis is based on N-body simulations, we can reproduce small scale structure as well, which permits us to obtain meaningful results by choosing smaller values for  $R$ .

Based on  $\delta$  calculated by the procedures above, we compute the statistical quantities, i.e., the dispersion, skewness and kurtosis for 6 time slices ( $z = 5, 4, 3, 2, 1, 0$ ). In order to obtain the statistical quantities, we generate 10 samples for the primordial density fluctuations by COSMICS for each dark energy model.

It is worth noting that we normalized the amplitude of the density spectrum at recombination era here, while the linear density spectrum is normalized by density dispersion at present era in other analyses like [22, 23, 24, 25]. Therefore in the nonlinear regime, our results seem different from theirs. However, as we show later, when  $w$  approaches to 0, the growth of the fluctuation is suppressed, which is consistent to them.

## 5. Numerical results

For comparison to the previous results, we set  $R = 8h^{-1}$  Mpc in the comoving Eulerian coordinates at the present time ( $a = 1$ ). In the previous paper, since we applied Lagrangian linear perturbation, we must examine the degree of the validity of the perturbative approach.

### (a) Validity of Lagrangian linear perturbation

**Table 2.** The difference of the dispersion, skewness, and kurtosis between Lagrangian linear perturbation and N-body simulations at  $z = 2$  ( $R = 8h^{-1}$  Mpc).

$w$	dispersion	skewness	kurtosis
-0.5	6.7%	-23.4%	-45.7%
-0.8	-1.6%	-24.7%	-47.8%
-0.9	-2.5%	-24.8%	-48.0%
-1.0	-3.0%	-25.0%	-48.2%
-1.2	-3.6%	-25.1%	-48.4%

At first, we compare the dispersion of the density distribution obtained by Lagrangian linear perturbation and N-body simulations. Figure 1 shows the time evolution of the dispersions of the density distribution for  $w = -1.0$ . In the early stages, since the evolution is well described by the linear theory, the dispersions based on the two methods are almost the same. For example, the difference is less than 0.7% at  $z = 5$ . In our previous paper, we compare non-Gaussianity of the density distribution at  $z = 2$  where the difference becomes a little larger, about 3%.

Even though the difference between Lagrangian linear perturbation and N-body simulations is still small until  $z = 2$  for the dispersion, it is not shown to hold also for non-Gaussianity of the density distribution. Figs. 2 and 3 show the time evolution of the skewness and kurtosis of the density distribution for  $w = -1$ , respectively and the difference is about 25% for the skewness and about 50% for the kurtosis. Therefore, it can be deduced that non-Gaussianity of the density distribution tend to be underestimated by Lagrangian linear perturbation, even for the region where the evolution of the dispersion is well described by it.

Regardless of the fact above, the conclusion of our previous paper that the difference of non-Gaussianity between  $w = -1$  and  $w = -0.8$  or  $-1.2$  is about 1% at  $z = 2$  remains unchanged, since the difference between Lagrangian linear perturbation and N-body simulations is also about 25% for the skewness and about 50% for the kurtosis for  $w = -0.8$  or  $-1.2$ . We summarize the difference of the statistical quantities between Lagrangian linear perturbation and N-body simulations at  $z = 2$  for various  $w$  (Table 2).

### (b) Statistical quantities ( $R = 8h^{-1}$ Mpc)

Next we compare the dispersion in several dark energy models based on N-body simulations. Now that we are using N-body simulations, we can go into the strongly nonlinear regime. Figure 4 shows the time evolution of the dispersion of the density distribution in several dark energy models. The growth of the dispersion monotonously continues until  $z = 0$ . The tendency of the dispersion among dark energy models is similar to that obtained by Lagrangian linear perturbation. As the value of  $w$  becomes larger (approaches zero), the dispersion becomes smaller. This can be explained as follows: for the model with larger  $w$ , dark energy dominates at an earlier era, and the expansion of the Universe starts accelerating earlier, while it can be shown that



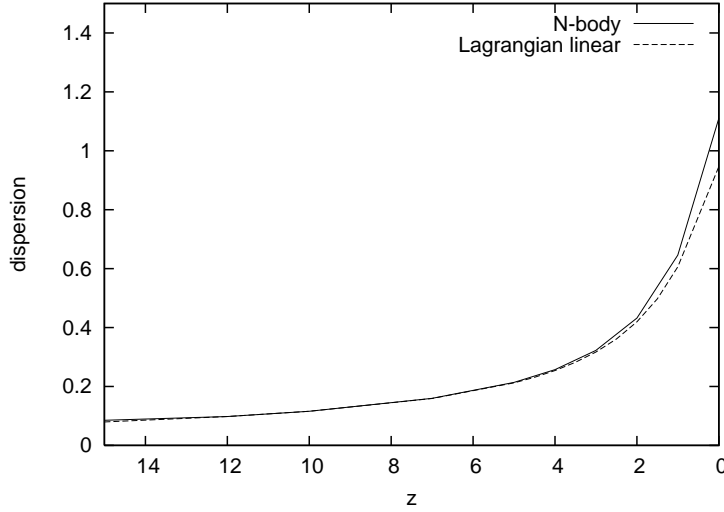


**Figure 1.** The dispersion of the density distribution based on Lagrangian linear perturbation and N-body simulations ( $R = 8h^{-1}\text{Mpc}$ ) for  $w = -1$ . Lagrangian linear perturbation keeps to be a good approximation until  $z \sim 2$ .

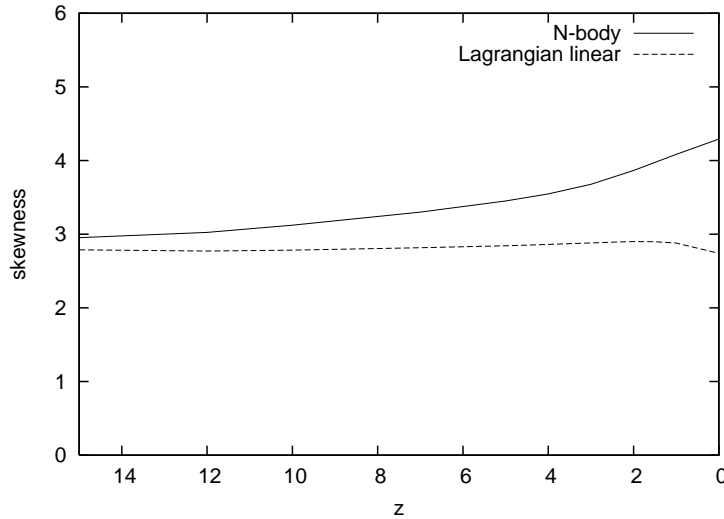


**Figure 2.** The skewness of the density distribution based on Lagrangian linear perturbation and N-body simulations ( $R = 8h^{-1}\text{Mpc}$ ) for the case of  $w = -1$ . The difference of the skewness which is already about 5% at  $z = 15$  increases.

the growth of the density fluctuation is slower in the accelerating stage than in the matter-dominant stage.

Figs. 5 and 6 show the time evolution of the skewness and kurtosis of the density distribution, respectively. It is different from that of the dispersion, in that the growth of them are not monotonous, especially after  $z = 1$ . Even though until  $z = 1$ , like the dispersion, these quantities are smaller as the value of  $w$  becomes larger, this order does not hold at the late time. Except the case  $w = -0.5$  whose dispersion is not large enough, they are larger as the value of  $w$  becomes larger.

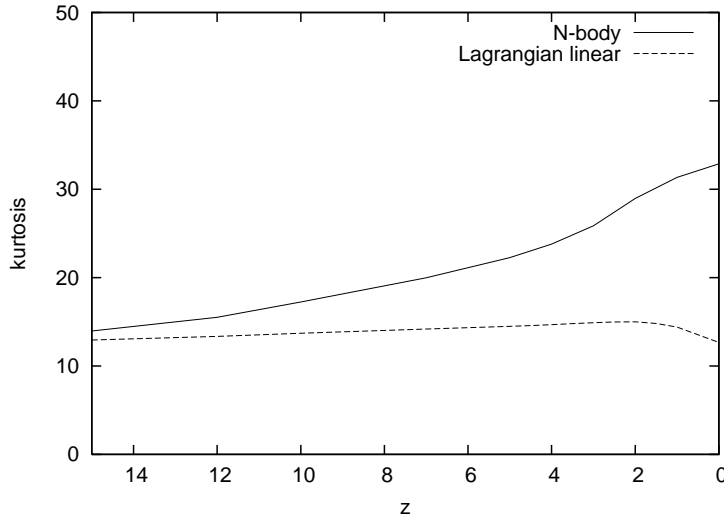


**Figure 3.** The Kurtosis of the density distribution based on Lagrangian linear perturbation and N-body simulations ( $R = 8h^{-1}\text{Mpc}$ ) for the case of  $w = -1$ . The difference of the kurtosis which is already about 7% at  $z = 15$  increases.

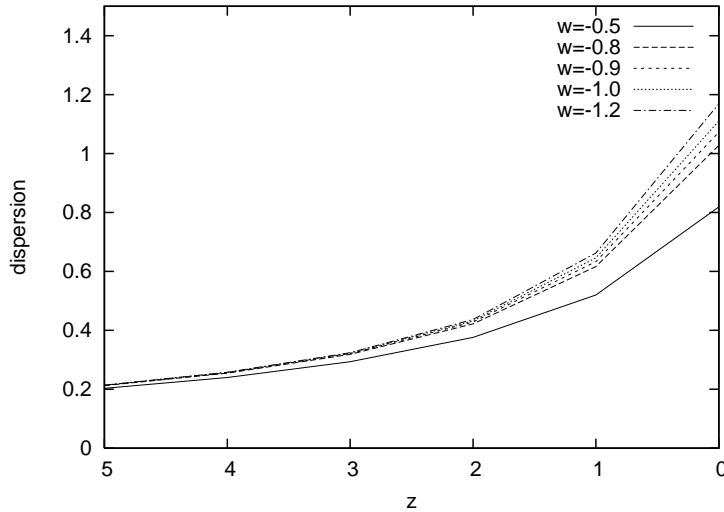


**Figure 4.** The dispersion of the density distribution in several dark energy models ( $R = 8h^{-1}\text{Mpc}$ ). The growth of the dispersion continues monotonously. As the value of  $w$  becomes larger (approaches zero), the dispersion becomes smaller. The difference of the dispersion between  $w = -1$  and  $w = -0.8$  is about 2.4% at  $z = 2$ , and become as large as 7.5% at  $z = 0$ . In the same way, the difference of the dispersion between  $w = -1$  and  $w = -1.2$  is 1.0% at  $z = 2$  and 5.3% at  $z = 0$ . The difference between  $w = -1$  and  $w = -0.5$  is already 13% at  $z = 2$ .

The detailed difference of the dispersion, skewness, and kurtosis for  $R = 8h^{-1}\text{Mpc}$  between  $w = -1.0$  and other  $w$  at  $z = 2$  and  $z = 0$  are summarized in tables 3 and 4, respectively.

Regardless of the change of the order of the  $w$  dependence, the differences of both the skewness and the kurtosis among  $w = -1.2$ ,  $w = -1$  and  $w = -0.8$  are much less

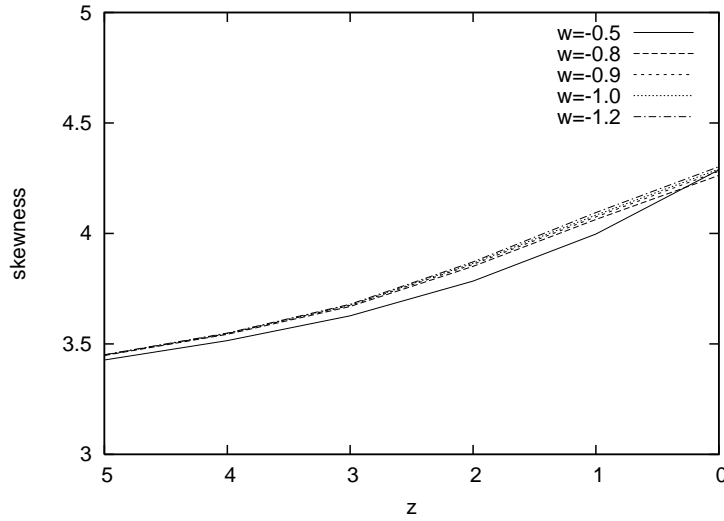


**Figure 5.** The skewness of the density distribution in several dark energy models ( $R = 8h^{-1}\text{Mpc}$ ). The skewness oscillate between  $z = 1$  and  $z = 0$ . We can easily distinguish the case for  $w = -0.5$  from the results. The difference of the skewness between  $w = -1$  and  $w = -0.8$  is about 0.4% at  $z = 2$ , then spreads out about 0.7% at  $z = 0$ . In the same way, the difference of the skewness between  $w = -1$  and  $w = -1.2$  is about 0.2% at  $z = 2$ , then spreads out about 0.3% at  $z = 0$ .

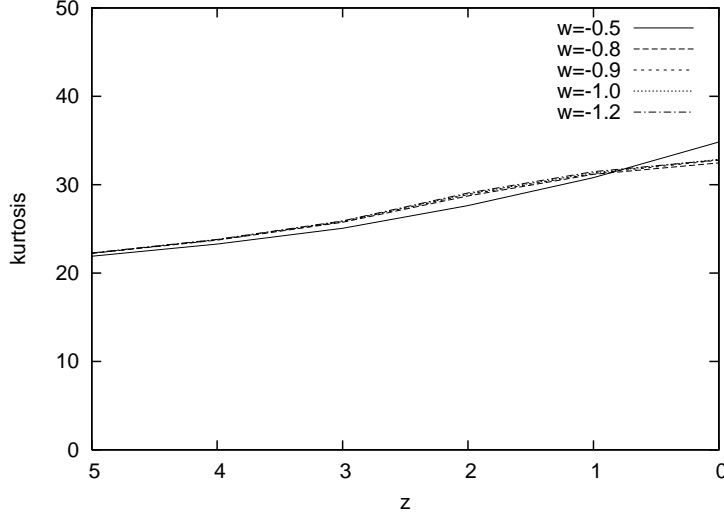


**Figure 6.** The kurtosis of the density distribution in several dark energy models ( $R = 8h^{-1}\text{Mpc}$ ). The kurtosis oscillate between  $z = 1$  and  $z = 0$ . As well as the skewness, the difference of the kurtosis between  $w = -1$  and  $w = -0.8$  is about 0.8% at  $z = 2$ , then spreads out about 1.2% at  $z = 0$ . In the same way, the difference of the kurtosis between  $w = -1$  and  $w = -1.2$  is about 0.3% at  $z = 2$ , then contract to about 0.2% at  $z = 1$ .

than 1% at  $z = 2$  but turn out to become as large as 1% (skewness) and 2% (kurtosis) at  $z = 0$ . For the case of  $w = -0.5$ , the values of both the skewness and the kurtosis are obviously less than that for the case of  $w = -1.0$  even at  $z = 2$  (about 2% and about

**Table 3.** The difference of the dispersion, skewness, and kurtosis between  $w = -1.0$  and other  $w$  at  $z = 2$  ( $R = 8h^{-1}$  Mpc).

$w$	dispersion	skewness	kurtosis
-0.5	-13.1%	-2.1%	-4.6%
-0.8	-2.4%	-0.37%	-0.80%
-0.9	-0.93%	-0.14%	-0.32%
-1.2	1.0%	0.15%	0.34%

**Table 4.** The difference of the dispersion, skewness, and kurtosis between  $w = -1.0$  and other  $w$  at  $z = 0$  ( $R = 8h^{-1}$  Mpc).

$w$	dispersion	skewness	kurtosis
-0.5	-26.2%	-0.09%	6.0%
-0.8	-7.5%	-0.67%	-1.2%
-0.9	-3.4%	-0.24%	-0.31%
-1.2	5.3%	0.25%	-0.19%

5%, respectively).

### (c) Statistical quantities ( $R = 2h^{-1}$ Mpc)

In this paper, since we apply N-body simulations, we can analyze smaller structure. In other words, even if we choose smaller value for  $R$ , we can obtain reliable results. Therefore, next we set the smoothing length  $R = 2h^{-1}$ Mpc in the comoving Eulerian coordinates at the present time ( $a = 1$ ). Even though the nonlinearity in this scale at  $z = 0$  is so strong that the corresponding galaxy distribution is influenced by the processes other than gravity such as the bias related with galaxy formation, it is worth investigating whether there exist other kind of scaling between higher order cumulants and the dispersion of the density distribution in this region.

Figure 7 shows the time evolution of the dispersion of the density distribution in several dark energy models. The tendency for the growth of the dispersion is similar to that for  $R = 8h^{-1}$ Mpc. The dispersion monotonously grows until  $z = 0$  and if the equation of state of dark energy  $w$  increases, the dispersion would decrease. Since we choose smaller smoothing scale, the dispersion is larger than that in the case of  $R = 8h^{-1}$ Mpc for a fixed  $z$  and  $w$ .

Figs. 8 and 9 show the time evolution of the skewness and kurtosis of the density distribution, respectively. As in the case of  $R = 8h^{-1}$ Mpc, the growth of them is not monotonous. It is shown that after  $z = 1$  for a fixed  $z$ , the skewness and kurtosis increases if the equation of state of dark energy  $w$  increases including the case  $w = -0.5$ . This suggests that in sufficiently nonlinear region, say  $\sigma > 2$ , there exists some scaling between the higher order cumulants and the dispersion  $\langle \delta^n \rangle_c \propto \sigma^{p(n)}$ , where  $p(n) < 2n - 2$ , at least inside the scope of our calculations.

The detailed difference of the dispersion, skewness, and kurtosis for  $R = 2h^{-1}$ Mpc

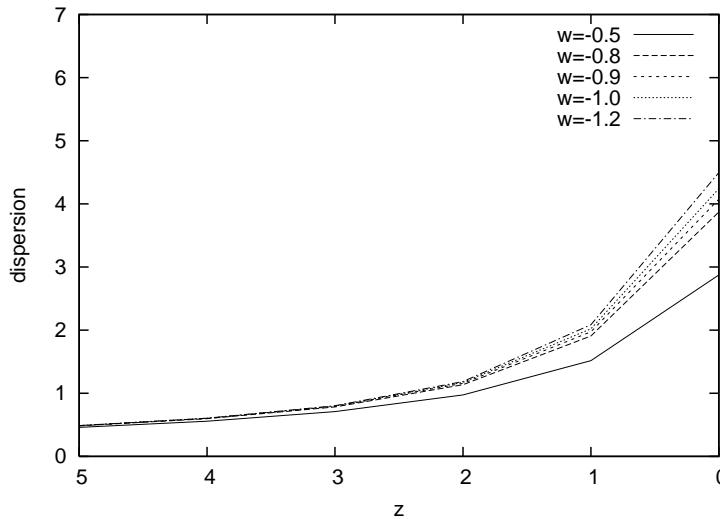


**Figure 7.** The dispersion of the density distribution in several dark energy models ( $R = 2h^{-1}\text{Mpc}$ ). The tendency of the difference of the dispersion is similar to that in the case of  $R = 8h^{-1}\text{Mpc}$ . The difference of the dispersion between  $w = -1$  and  $w = -0.8$  is about 8.7% at  $z = 0$ . Similarly the difference of the dispersion between  $w = -1$  and  $w = -1.2$  is about 6.0% at  $z = 0$ . The difference of the dispersion between  $w = -1$  and  $w = -0.5$  is quite large (about 17% already at  $z = 2$ ).

**Table 5.** The difference of the dispersion, skewness, and kurtosis between  $w = -1.0$  and other  $w$  at  $z = 2$  ( $R = 2h^{-1}\text{ Mpc}$ ).

$w$	dispersion	skewness	kurtosis
-0.5	-16.8%	-7.8%	-13.0%
-0.8	-3.1%	-1.2%	-1.9%
-0.9	-1.2%	-0.48%	-0.81%
-1.2	1.3%	0.53%	0.97%

between  $w = -1.0$  and other  $w$  at  $z = 2$  and  $z = 0$  are summarized in tables 5 and 6, respectively.

Regardless of the change of the order of the  $w$  dependence, the differences of both the skewness and the kurtosis among  $w = -1.2$ ,  $w = -1$  and  $w = -0.8$  are much less than 2% at  $z = 2$  but turn out to become as large as 3% (skewness) and 9% (kurtosis) at  $z = 0$ . For the case of  $w = -0.5$ , the values of both the skewness and the kurtosis are obviously less than that for the case of  $w = -1.0$  even at  $z = 2$  (about 8% and about 13%, respectively).

#### (d) Probability distribution function

In order to clarify the difference between the case of  $w = -0.8$  and  $w = -1.0$ , we present raw data of PDF of the density distribution at  $z = 0$  for  $R = 8h^{-1}\text{Mpc}$  (Figure 10), and  $R = 2h^{-1}\text{Mpc}$  (Figure 11), respectively. When the nonlinear effect promotes the formation of the dense structure and restrains the evolution of the voids,

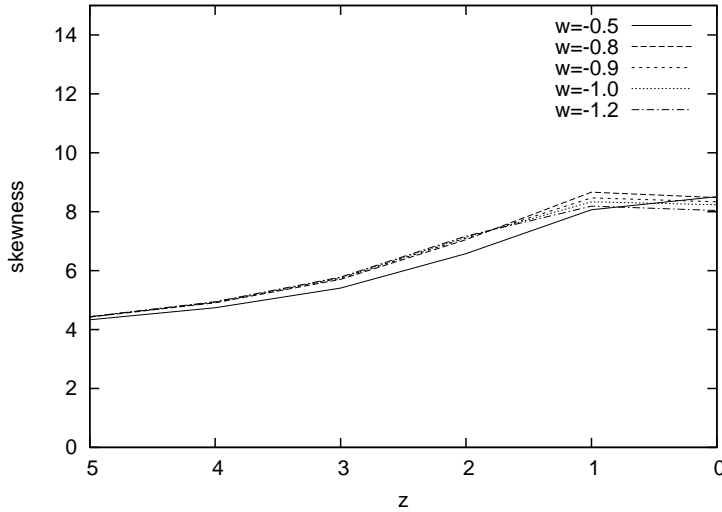


**Figure 8.** The skewness of the density distribution in several dark energy models ( $R = 2h^{-1}\text{Mpc}$ ). The growth of the skewness stops after  $z = 1$ . The difference of the skewness between  $w = -1$  and  $w = -0.8$  is about 3.0% at  $z = 0$ . At some time between  $z = 1$  and  $z = 0$ , the skewness of  $w = -0.8$  becomes larger than that of  $w = -1.0$ . In the same way, the difference between  $w = -1$  and  $w = -1.2$  is about 2.4% at  $z = 0$ . At some time between  $z = 1$  and  $z = 0$ , the skewness of  $w = -1.2$  becomes smaller than that of  $w = -1.0$ . The difference between  $w = -1$  and  $w = -0.5$  is as large as 3.4% even at  $z = 0$ .

**Table 6.** The difference of the dispersion, skewness, and kurtosis between  $w = -1.0$  and other  $w$  at  $z = 0$  ( $R = 2h^{-1}$  Mpc).

$w$	dispersion	skewness	kurtosis
-0.5	-32.2%	3.4%	7.7%
-0.8	-8.7%	3.0%	4.5%
-0.9	-3.9%	1.2%	2.6%
-1.2	6.0%	-2.4%	-9.0%

the degree of asymmetry of PDF (skewness) grows obviously. On the other hand, if the edge of PDF spreads widely without reduction of peak, the “peakiness” of PDF (kurtosis) grows evidently.

### (e) Error analysis

Until now, we provided our results without error bars, even though they are obtained by averaging 10 samples for each dark energy model. However, in order to check whether these results can be used directly as a cosmological tool, the statistical error analysis is necessary. Here we estimate the variances among samples for the case of  $w = -1.0$  by increasing the number of samples up to 50. The results are showed in Figs. 12-14. As a result, contrary to our expectation, the variance is much larger than the difference between the difference of the non-Gaussianity between  $w = -1$  and the other cases. Furthermore, it turns out that although the variance of the dispersion can be

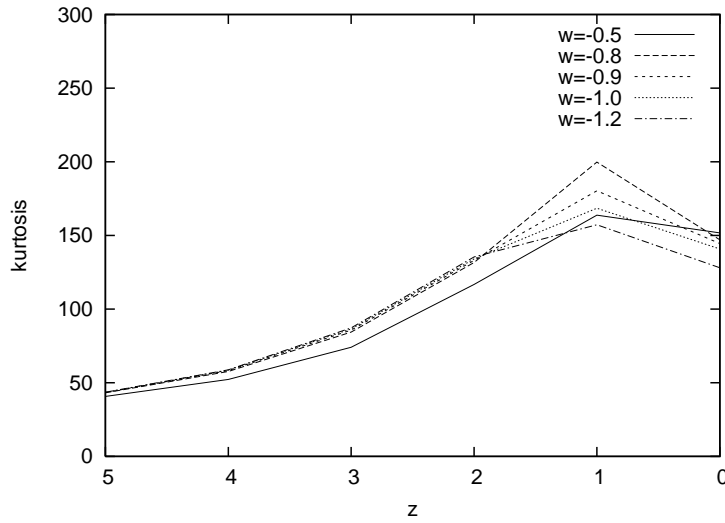


**Figure 9.** The kurtosis of the density distribution in several dark energy models ( $R = 2h^{-1}\text{Mpc}$ ). The growth of the kurtosis stops at  $z = 1$ . The difference of the kurtosis between  $w = -1$  and  $w = -0.8$  is about 4.5% at  $z = 0$ . At some time between  $z = 1$  and  $z = 0$ , the kurtosis of  $w = -0.8$  becomes larger than that of  $w = -1.0$ . In the same way, the difference between  $w = -1$  and  $w = -1.2$  is about 9% at  $z = 0$ . At some time around  $z = 2$ , the kurtosis of  $w = -1.2$  becomes smaller than that of  $w = -1.0$ . The difference between  $w = -1$  and  $w = -0.5$  is as large as 8% even at  $z = 0$ .

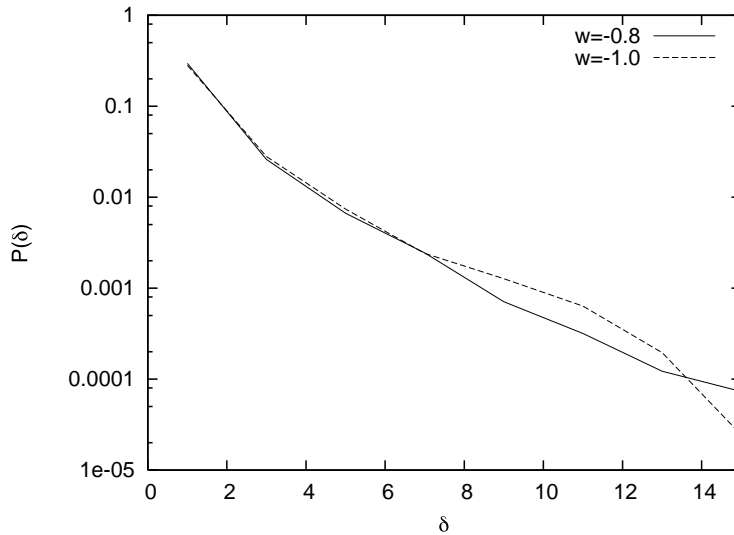


**Figure 10.** The PDF of the density distribution in  $w = -0.8$  and  $w = -1.0$  at  $z = 0$  ( $R = 8h^{-1}\text{Mpc}$ ). Because of smoothing for the PDF, we pick up the PDF with low resolution ( $\Delta\delta = 2$ ). Since the PDF of  $w = -1.0$  spreads more widely than that of  $w = -0.8$  for almost the same dispersion, the non-Gaussianity of the PDF of  $w = -1.0$  is larger than that of  $w = -0.8$ .

decreased, the variance of the non-Gaussianity is not necessarily improved by increasing the number of samples. The detailed results are shown in Figs. 12-14. Therefore, for the practical use of this analysis to constrain the dark energy models, further improvements

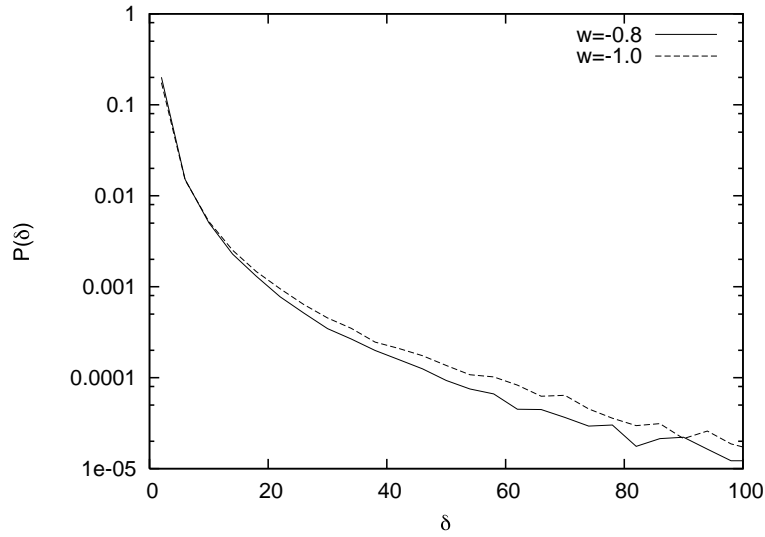


**Figure 11.** The PDF of the density distribution in  $w = -0.8$  and  $w = -1.0$  at  $z = 0$  ( $R = 2h^{-1}$  Mpc). Because of smoothing for the PDF, we pick up the PDF with low resolution ( $\Delta\delta = 4$ ). Even though the PDF of  $w = -1.0$  spreads more widely than that of  $w = -0.8$ , since the dispersion of the PDF of  $w = -1.0$  is larger than that of  $w = -0.8$ , the resulting non-Gaussianity becomes smaller for the case of  $w = -1.0$ .

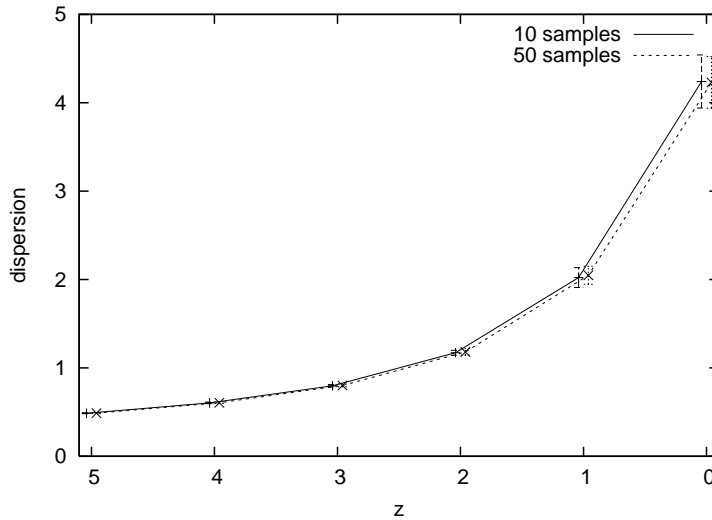


**Figure 12.** The dispersion of the density distribution in the case of  $w = -1.0$  ( $R = 2h^{-1}$  Mpc). Here we analyze the variance of samples. When we increase number of samples, the variance slightly decreases. The variance is about 7% at  $z = 0$  in both cases.

for the calculation of the statistical quantities, which seems to be worth considering is necessary.



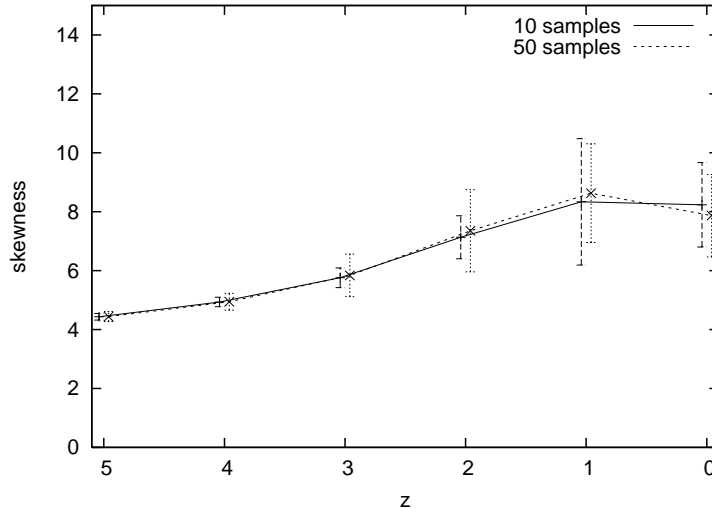


**Figure 13.** The skewness of the density distribution in the case of  $w = -1.0$  ( $R = 2h^{-1}\text{Mpc}$ ). Here we analyze the variance of samples. Even if we increase number of samples, the variance of the non-Gaussianity is not always improved. The variance is about 18% at  $z = 0$ .

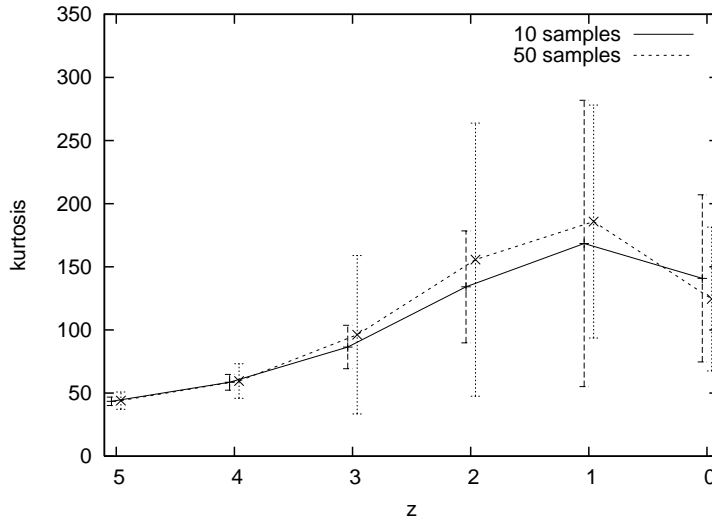


**Figure 14.** The kurtosis of the density distribution in the case of  $w = -1.0$  ( $R = 2h^{-1}\text{Mpc}$ ). Here we analyze the variance of samples. Even if we increase number of samples, the variance of the non-Gaussianity is not always improved. The variance is about 46% at  $z = 0$ .

## 6. Summary

To clarify the nature of dark energy is, without doubt, one of the most important tasks in modern cosmology. From the phenomenological viewpoint, it is important to constrain the effective equation of state of dark energy  $w$  by observations. Even though we have obtained the constraint as  $w < -0.90$  (95 % confidence limit assuming  $w \geq -1$ ) [11] by combining WMAP data with other astronomical data, to pin down the value of  $w$ , it is

necessary to propose other independent observational tools.

For this purpose, we consider non-Gaussianity of the density distribution which is generated by the non-linear dynamics. In this paper, as a natural extension to our previous work [13] where we follow a semi-analytic approach based on Lagrangian linear perturbation theory, we apply N-body simulations based on  $P^3M$  codes. In terms of the density fluctuation obtained by N-body simulations, we compute the skewness and kurtosis of the smoothed density distribution with the appropriate definition in that they become constant in extremely weakly nonlinear stage. They are important statistical quantities denoting the deviation from the Gaussian distribution. By considering several constant- $w$  dark energy models ( $w = -0.5, -0.8, -0.9, -1.0, -1.2$ ), we present the  $w$ -dependence of the time evolution of non-Gaussianity of the density distribution.

First we compare the results for the weakly nonlinear region at  $z = 2$  obtained by N-body simulations and Lagrangian linear perturbation by choosing the same smoothing length  $R = 8h^{-1}$  Mpc. In this region where non-Gaussianity become smaller as  $w$  becomes larger, we regarded the results by Lagrangian linear perturbation as reliable in the previous work. As a result, even though the dispersion obtained by Lagrangian linear perturbation agrees well with the ones obtained by N-body simulations until  $z \sim 2$ , non-Gaussianity tend to be underestimated by Lagrangian linear perturbation.

This result is attributed to the fact that second order Lagrangian perturbation is necessary to express second order Eulerian perturbation [37, 38], mathematically and the peculiar acceleration perpendicular to the peculiar velocity can not be picked up by Lagrangian linear perturbation, physically. Therefore, we learn the fact that ‘‘Lagrangian linear perturbation is not necessarily better than second order Eulerian perturbation’’. However, regardless of the underestimation of non-Gaussianity, the conclusions of the previous paper that the relative difference of non-Gaussianity between  $w = -1.0$  and  $w = -0.8$  or  $w = -1.2$  is about 1% at  $z = 2$  for  $R = 8h^{-1}$ Mpc remains unchanged because the degree of the underestimation in Lagrangian linear perturbation is almost  $w$ -independent.

Next, we analyze the statistical quantities in the strongly nonlinear region where the previous perturbative approach is obviously invalid. We find that the relative difference of non-Gaussianity among several constant- $w$  models spread as  $z \rightarrow 0$ , even though the growth of non-Gaussianity is not monotonous in that region and the order changes around  $z = 0.5$  except  $w = -0.5$  model whose dispersion is not so large enough. For example, at  $z = 0$  the relative difference between non-Gaussianity of  $w = -0.8$  model and that of  $w = -1.0$  model is 0.67% for the skewness and 1.2% for the kurtosis, while at  $z = 2$  they are  $-0.52\%$  for the skewness and  $-1.3\%$  for the kurtosis. Similarly, at  $z = 0$  the difference between non-Gaussianity of  $w = -1.2$  model and that of  $w = -1.0$  model is 0.25% for the skewness and  $-0.19\%$  for the kurtosis, while at  $z = 2$  they are 0.15% for the skewness and 0.34% for the kurtosis.

Making use of N-body simulations, we also analyze the smaller structure by setting the smoothing scale  $R = 2h^{-1}$ Mpc, even though the nonlinearity in this scale at  $z = 0$  is so strong that the galaxy distribution is influenced by the process other than gravity.

For this case, since we look at the smaller scale, the dispersion and non-Gaussianity of the density distribution is larger than that in the case of  $R = 8h^{-1}\text{Mpc}$  for a fixed  $z$  and  $w$ . Relative difference of non-Gaussianity among several constant- $w$  models are also greater than the case of  $R = 8h^{-1}\text{Mpc}$ .

For example, at  $z = 0$  the relative difference between non-Gaussianity of  $w = -0.8$  model and that of  $w = -1.0$  model is 3.0% for the skewness and 4.5% for the kurtosis. Similarly, the relative difference between the non-Gaussianity of  $w = -1.2$  model and that of  $w = -1.0$  model is -2.4% for the skewness and -9.0% for the kurtosis. Furthermore, on the contrary to the weakly nonlinear region, for a fixed  $z$  we confirm non-Gaussianity become larger as  $w$  becomes larger after  $z = 0.5$ , including the case of  $w = -0.5$ .

This suggests that in the sufficiently nonlinear region, say  $\sigma > 2$ , there exists some scaling between the higher order cumulants and the dispersion  $\langle \delta^n \rangle_c \propto \sigma^{p(n)}$ , where  $p(n) < 2n - 2$ , at least inside the scope of our calculations. Academically, not limited to the constraint for the dark energy models, this result seems to worth investigating related with the nature of the nonlinear gravitational clustering in the expanding Universe.

It is necessary to mention the possibility of examining our results. Recently, several galaxy redshift survey projects have been progressing [39, 40, 41]. In these projects, many galaxies within a region ( $z < 0.3$  for 2dF,  $z < 0.5$  for SDSS, and  $0.7 < z < 1.4$  for DEEP2) have been observed. These projects show the latest distribution of galaxies, which form strongly nonlinear structure. Actually, the skewness and kurtosis of the distribution of SDSS Early Data Release had been computed [42]. The results suggested the SDSS imaging data can enable to determine the skewness and kurtosis up to 1% and less than 10%, respectively. Therefore, in future projects we can expect to determine the skewness and kurtosis with high accuracy. However, based on our error analysis, the variance of the non-Gaussianity turned out to be about 50% for 10 samples and it does not increased even by increasing the number of samples up to 50. This suggests that our analysis, by itself, is still immature and further improvements are necessary for the practical use to constrain the property of dark energy.

As mentioned above, for smaller scale like  $R = 2h^{-1}\text{Mpc}$  now, the complex physical processes about galaxy formation affect the galaxy distribution. In order to use observational data such as the PSCz survey [43] which is an all sky survey at the present epoch, it is necessary to create mock PSCz catalogs from our results making use of the PSCz selection function [44]. Even though this is from excessively academical interest,  $w$ -dependence of the non-Gaussianity of the actual galaxy distribution seems to be worth investigating. On the other hand, it is known that weak lensing surveys can potentially provide us with precision maps of the projected density up to redshifts around 1 [45, 46, 47, 48]. Even though we need another step of obtaining the convergence field which can be written as the projection of the matter density along the line of sight, the skewness and kurtosis of the convergence field can be tested by weak lensing surveys. Obviously, our results obtained in this paper help to derive these quantities.

Finally, it is worth noting that primordial non-Gaussianity which is generated by

inflation [29]. From WMAP observations, a limit for the non-linear coupling parameter has been established [49] which does not deny the existence of non-Gaussianity in the primordial density fluctuations. Even though we cannot disentangle them generally, we can calculate non-Gaussianity of large scale structure for a given non-Gaussian initial condition and compare the results with the one obtained by the Gaussian initial condition. This requires further investigations and we hope to report results in a separate publication.

## Acknowledgments

We thank to Masahiro Morikawa for useful discussion. For usage of COSMICS and  $P^3M$  codes, we would like to thank Edmund Bertschinger and Alexander Shirokov. SM is supported in part by the Japan Society for Promotion of Science (JSPS) Research Fellowship.

## References

- [1] Peebles P J E 1980 *The Large-Scale Structure of the Universe* (Princeton: Princeton University Press)
- [2] Peacock J 1999 *Cosmological Physics* (Cambridge: Cambridge University Press)
- [3] Liddle A R and Lyth D H 2000 *Cosmological Inflation and Large-Scale Structure* (Cambridge: Cambridge University Press)
- [4] Coles P and Lucchin F 2002 *Cosmology, The Origin and Evolution of Cosmic Structure* (Chichester, John Wiley)
- [5] Starobinsky A A 1982 *Phys. Lett. B* **117** 175
- [6] Kofman L, Bertschinger E, Gelb J M, Nusser A and Dekel A 1994 *Astrophys. J.* **420** 44
- [7] Ueda H and Yokoyama J 1996 *Mon. Not. R. Astron. Soc.* **280** 754
- [8] Perlmutter S *et al.* 1999 *Astrophys. J.* **517** 565; Riess A G 1998 *Astron. J* **116** 1009
- [9] Bennett C L *et al.* 2003 *Astrophys. J. Supp.* **148** 1
- [10] Tegmark M *et al.* 2004 *Astrophys. J.* **606** 702
- [11] Spergel D N *et al.*, [arXiv:astro-ph/0603449].
- [12] Weinberg S 1989 *Rev. Mod. Phys.* **61** 1; Sahni V and Starobinsky A A 2000 *Int. J. Mod. Phys. D* **9** 373; Copeland E J, Sami M and Tsujikawa S, [arXiv:hep-th/0603057].
- [13] Tatekawa T and Mizuno S 2006 *JCAP* **02** 006
- [14] Plionis M, Borgani S, Moscardini L, and Coles P 1995 *Astrophys. J.* **441** L57
- [15] Borgani S, Plionis M, Coles P, and Moscardini L 1995 *Mon. Not. R. Astron. Soc.* **277** 1191
- [16] Kayo I, Taruya A, and Suto Y 2001 *Astrophys. J.* **561** 22
- [17] Zel'dovich Ya B 1970 *Astron. Astrophys.* **5** 84
- [18] Arnol'd V I, Shandarin S F, and Zel'dovich Ya B 1982 *Geophys. Astrophys. Fluid Dynamics* **20** 111
- [19] Tatekawa T 2005 *Recent Res. Devel. Astrophys.* **2** 1 [arXiv:astro-ph/0412025].
- [20] Munshi D, Sahni V and Starobinsky A A 1994 *Astrophys. J.* **436** 517 [arXiv:astro-ph/9402065].
- [21] Yoshisato A, Matsubara T and Morikawa M 1998 *Astrophys. J.* **498** 48 [arXiv:astro-ph/9707296]
- [22] Linder E V and Jenkins A 2003 *Mon. Not. Roy. Astron. Soc.* **346** 573 [arXiv:astro-ph/0305286].
- [23] Klypin A, Maccio A V, Mainini R and Bonometto S A 2003 *Astrophys. J.* **599** 31 [arXiv:astro-ph/0303304].
- [24] Kuhlen M, Strigari L E, Zentner A R, Bullock J S and Primack J R 2005 *Mon. Not. Roy. Astron. Soc.* **357** 387 [arXiv:astro-ph/0402210].

- [25] McDonald P, Trac H and Contaldi C 2006 *Mon. Not. Roy. Astron. Soc.* **366** 547 [arXiv:astro-ph/0505565].
- [26] Coble K, Dodelson S and Frieman J A 1997 *Phys. Rev.* **D55** 1851 [arXiv:astro-ph/9608122].
- [27] Caldwell R R, Dave R and Steinhardt P J 1998 *Phys. Rev. Lett.* **80** 1582 [arXiv:astro-ph/9708069].
- [28] However, it must be worth noting that the small deviation from Gaussian perturbation at primordial time become one of the main topic for the research of Early Universe, see for example [29]
- [29] Bartolo N, Komatsu E, Matarrese S and Riotto A 2004 *Phys. Rep.* **402** 103 [arXiv:astro-ph/0406398].
- [30] Bernardeau F, Colombi S, Gaztañaga E and Scoccimarro R 2002 *Phys. Rept.* **367** 1
- [31] Kamionkowski M and Buchalter A 1999 *Astrophys. J.* **514** 7 [arXiv:astro-ph/9807211].
- [32] Gaztanaga E and Lobo J A 2001 *Astrophys. J.* **548** 47 [arXiv:astro-ph/0003129].
- [33] Benabed K and Bernardeau F 2001 *Phys. Rev.* **D64** 083501 [arXiv:astro-ph/0104371].
- [34] Hockney R W and Eastwood W 1981 *Computer Simulation Using Particles* (New York: McGraw-Hill); Bertschinger E and Gelb J M 1991 *Computers in Physics* Mar/Apr, 164
- [35] Ma C P and Bertschinger E 1995 *Astrophys. J.* **455** 7
- [36] Basilakos S and Plionis M, [arXiv:astro-ph/0607065].
- [37] Grinstein B and Wise M B 1987 *Astrophys. J.* **320** 448
- [38] Bouchet F R, Juszkiewicz R, Colombi S and Pellat R 1992 *Astrophys. J.* **394** L5
- [39] Hawkins Ed *et al.* 2003 *Mon. Not. R. Astron. Soc.* **346** 78
- [40] Abazajian K *et al.* 2005 *Astron. J.* **129** 1755
- [41] Gerke B F 2005 *Astrophys. J.* **625** 6
- [42] Szapudi I *et al.* [SDSS Collaboration] 2002 *Astrophys. J.* **570** 75 [arXiv:astro-ph/0111058].
- [43] W. Saunders *et al.*, *Mon. Not. Roy. Astron. Soc.* **317**, 55 (2000) [arXiv:astro-ph/0001117].
- [44] M. Rowan-Robinson *et al.*, *Mon. Not. Roy. Astron. Soc.* **314**, 375 (2000) [arXiv:astro-ph/9912223].
- [45] van Waerbeke L *et al.* 2000 *Astron. Astrophys.* **358** 30 [arXiv:astro-ph/0002500].
- [46] Bacon D J, Refregier A R and Ellis R S 2000 *Mon. Not. Roy. Astron. Soc.* **318** 625 [arXiv:astro-ph/0003008].
- [47] Wittman D M, Tyson J A, Kirkman D, Dell'Antonio I and Bernstein G 2000 *Nature* **405** 143 [arXiv:astro-ph/0003014].
- [48] Kaiser N, Wilson G and Luppino G A, [arXiv:astro-ph/0003338].
- [49] Komatsu E *et al.* 2003 *Astrophys. J. Suppl.* **148** 119 [arXiv:astro-ph/0302223].